Molecular Therapy
Oncology
Original Article

Empowering pancreatic tumor homing with augmented anti-tumor potency of CXCR2-tethered CAR-NK cells

Jong Hyeon Yoon,[1,10] Han-Na Yoon,[2,10] Hyun Ju Kang,[3,6,10] Hyejin Yoo,[1] Moon Jung Choi,[4] Joo-Yoon Chung,[1,9] Minkoo Seo,[5] Minsung Kim,[6] Si On Lim,[6] Yong Jun Kim,[8,9] Jin-Ku Lee,[3,6,7] and Mihue Jang[1,9]

[1]Medicinal Materials Research Center, Biomedical Research Division, Korea Institute of Science and Technology, Seoul 02792, Republic of Korea; [2]Rare & Pediatric Cancer Branch, Division of Rare and Refractory Cancer, Research Institute, National Cancer Center, Goyang 10408, Republic of Korea; [3]Genomic Medicine Institute, Medical Research Center, Seoul National University, Seoul 03080, Republic of Korea; [4]Division of Hematology and Oncology, Brown University, Providence, RI, USA; [5]Corporate Research & Development Center, UCI Therapeutics, Seoul 04784, Republic of Korea; [6]Department of Biomedical Sciences, Seoul National University College of Medicine, Seoul 03080, Republic of Korea; [7]Department of Anatomy and Cell Biology, Seoul National University College of Medicine, Seoul 03080, Republic of Korea; [8]Department of Pathology, College of Medicine, Kyung Hee University, Seoul 02447, Republic of Korea; [9]KHU-KIST Department of Converging Science and Technology, Kyung Hee University, Seoul 02447, Republic of Korea

Chimeric antigen receptor (CAR)-engineered natural killer (NK) cells are a promising immunotherapy for solid cancers; however, their effectiveness against pancreatic cancer is limited by the immunosuppressive tumor microenvironment. In particular, low NK cell infiltration poses a major obstacle that reduces cytotoxicity. The current study aimed to enhance the tumor-homing capacity of CAR-NK cells by targeting the chemokine-chemokine receptor axis between NK and pancreatic cancer cells. To this end, data from a chemokine array and The Cancer Genome Atlas pan-cancer cohort were analyzed. Pancreatic cancer cells were found to secrete high levels of ligands for C-X-C motif receptor 1 (CXCR1) and CXCR2. Subsequently, we generated anti-mesothelin CAR-NK cells incorporating CXCR1 or CXCR2 and evaluated their tumor-killing abilities in 2D cancer cell co-culture and 3D tumor-mimetic organoid models. CAR-NK cells engineered with CXCR2 demonstrated enhanced tumor killing and strong infiltration of tumor sites. Collectively, these findings highlight the potential of CXCR2-augmented CAR-NK cells as a clinically relevant modality for effective pancreatic cancer treatment. By improving their infiltration and tumor-killing capabilities, these CXCR2-augmented CAR-NK cells have the potential to overcome the challenges posed by the immunosuppressive tumor microenvironment, providing improved therapeutic outcomes.

INTRODUCTION

Pancreatic ductal adenocarcinoma (PDAC) is an extremely aggressive malignancy characterized by delayed diagnosis, primarily owing to its nonspecific clinical symptoms.[1,2] The efficacy of chemotherapies, such as FOLFIRINOX and gemcitabine, for PDAC remains limited, failing to significantly improve clinical outcomes.[3,4] This limited efficacy can be attributed to the unique tumor microenvironment (TME) prevalent in PDAC, characterized by a strong desmoplastic reaction. This promotes disease progression and contributes to chemotherapy resistance.[5] Notably, the highly immunosuppressive properties of the pancreatic TME restricts the effectiveness of immune cell-mediated anti-cancer therapies by hindering immune cell infiltration.

Natural killer (NK) cells serve as vital innate sentinels that rapidly eliminate abnormal cells, such as those infected by viruses or tumor cells, without needing prior sensitization.[6] Unlike T cells, NK cells possess unique cytotoxic capabilities and lack antigen-specific recognition. These attributes are governed by a delicate equilibrium between stimulatory and inhibitory receptor-mediated signaling, enabling the recognition of a diverse array of target cell ligands.[7] Recently, NK-based adoptive immunotherapy has emerged as a promising approach with extensive clinical potential.[8,9] An important advantage of such immunotherapy is the ability to utilize NK cells as off-the-shelf allogeneic products, independent of the need for specific gene modifications, thus facilitating large-scale manufacturing.[10,11] Furthermore, the use of chimeric antigen receptor (CAR)-engineered NK cells is associated with enhanced cytotoxicity and provides potential clinical applications with minimal adverse toxicities.[12,13] Compared with CAR-T cells, CAR-NK cells offer favorable clinical benefits by avoiding toxic side effects such as graft-vs.-host disease,[14] acute cytokine release syndrome, or immune cell-associated

Received 4 August 2023; accepted 15 February 2024;
https://doi.org/10.1016/j.omton.2024.200777.

[10]These authors contributed equally

Correspondence: Jin-Ku Lee, Genomic Medicine Institute, Medical Research Center, Seoul National University, Seoul 03080, Republic of Korea.
E-mail: jinkulee@snu.ac.kr
Correspondence: Mihue Jang, Medicinal Materials Research Center, Biomedical Research Division, Korea Institute of Science and Technology, Seoul 02792, Republic of Korea.
E-mail: mihue@kist.re.kr

neurotoxicity syndrome.[15] Thus, NK cell-based therapies hold considerable promise as a highly feasible and accessible therapeutic modality.

CAR-NK cells have been engineered as an attractive therapeutic option in preclinical studies to redirect their activity toward solid tumors.[16–18] However, despite these advancements, effectively targeting solid tumors remains challenging, accounting for the suboptimal outcomes. Notably, inadequate infiltration of NK cells significantly limits successful clinical outcomes, particularly for solid tumors.[19–23] The number and proportion of infiltrating NK cells are of particular prognostic significance in PDAC. Indeed, enhanced infiltration of NK cells within the TME correlates with delayed disease recurrence and serves as a positive prognostic marker.[24] Consequently, to improve the effectiveness of PDAC treatment, additional modifications that facilitate the infiltration of CAR-NK cells into pancreatic TME are required.

Chemokines are small inflammatory mediators with chemotactic properties critical in attracting immune cells to specific locations.[25] Chemokines are classified into four subgroups, namely CXC, CC, CX3C, and C, based on the position of the first two terminal cysteine residues.[26,27] They bind to specific G-protein-coupled seven-transmembrane receptors, facilitating the direct migration of immune cells to target sites via chemotaxis. This process involves the movement of cells along chemokine gradients. Recognizing the importance of increased intratumoral infiltration of NK cells, numerous studies have explored the possibility of enhancing their trafficking to specific tumor sites through genetic engineering. To date, specific chemokine receptors, including CCR5, CCR7, CXCR1, CXCR2, and CXCR4, have been engineered to enhance NK cell migration against various tumors including lymphoma, colon cancer, ovarian cancer, renal cell carcinoma, osteosarcoma, and glioblastoma.[19,28–34] However, that has been little research on advanced strategies involving CAR-NK cells that modulate chemokine receptors specific to pancreatic cancers. Therefore, our aim was to develop pancreatic cancer-directed CAR-NK cells, augmented with specific chemokine receptors, to enable tumor infiltration and effective anti-tumor immunity.

RESULTS

Chemokine secretion profiles of pancreatic cancer cells

To uncover the specific subset of chemokines secreted by pancreatic cancer cells that could act as mediators for NK cell targeting of tumor cells, we conducted a comprehensive human chemokine array using the supernatant collected from three pancreatic cancer cell lines, Capan-2, AsPC-1, and PANC-1 (Figures 1A, 1B, and S1). Additionally, we compared the chemokine secretion profiles in the human primary pancreatic stellate cells (HPaSteC) cell supernatant. The pancreatic cancer cell lines had high levels of secreted CXCL1, CXCL2, CXCL3, and CXCL8, which are chemokine ligands for CXCR1 or CXCR2.[35] CXCR1 predominantly binds to CXCL6 and CXCL8 (interleukin-8 [IL-8]) with high affinity, whereas CXCR2 interacts with seven CXC chemokines, namely CXCL1, CXCL2, CXCL3, CXCL5, CXCL6, CXCL7, and CXCL8, all of which share an ELR motif.[36] In contrast, the HPaSteC cell culture supernatant had comparatively lower levels of these chemokines (Figures 1A and 1B). Furthermore, we confirmed the expression of CXCR1 and CXCR2 ligands at the RNA and protein levels in pancreatic cancer cell extracts (Figures 1C and S2).

To gain further insights into the significance of CXCR1 and CXCR2 ligands in pancreatic cancers, we analyzed the gene score distribution of *CXCL1*, *CXCL2*, *CXCL3*, *CXCL5*, *CXCL6*, *CXCL7*, and *CXCL8* across various cancer types using The Cancer Genome Atlas (TCGA) pan-cancer cohort. Notably, pancreatic cancers exhibited higher scores for CXCR1 and CXCR2 ligands (Figure 1D). Patients with pancreatic cancer with high scores for CXCLs, including CXCR1 and CXCR2 ligands, exhibited poorer overall survival rates than those with low scores (Figure 1E). Taken together, our findings suggest that augmenting CXCR1 or CXCR2 expression in NK cells may result in promising clinical outcomes with improved anti-tumor activity by enhancing NK cell infiltration into pancreatic tumor sites.

Generation and characterization of CXCR1- and CXCR2-pNK cells and their characterization

We evaluated the expression of CXCR1–3 on the surface of resting pNK cells and *ex vivo* expanded pNK cells, obtained from peripheral blood mononuclear cells (PBMCs) collected from healthy donors, via flow cytometry analysis (Figures 2A, 2B, and S3). Both resting and expanded pNK cells exhibited relatively low expression of CXCR1 and CXCR2. However, high CXCR3 expression was observed in both cell populations. Subsequently, we generated CXCR1- or CXCR2-overexpressing pNK cells from healthy donor-derived PBMCs using lentiviral transduction (Figure 2C). High transduction efficiencies of 68.09% and 61.96% were achieved for CXCR1 and CXCR2, respectively (Figure 2D). These cells underwent a 15-day expansion period that incorporated a 5-day transduction phase. We then evaluated the transduction efficacy in long-term expanded NK cells from various donors (Figure S4). The transduction efficiencies remained consistent even in NK cells expanded for 22 days, including 12 days post-viral transduction. Subsequently, when examining the surface expression of NK-activating markers and the *in vitro* NK-mediated cancer killing against Capan-2, AsPC-1, and PANC-1 cells, no significant differences were observed between CXCR1- and CXCR2-augmented, and control pNK cells (Figures 2E and 2F). These findings indicated that the augmentation of CXCR1 or CXCR2 in pNK cells did not significantly affect their activity under *in vitro* 2D culture conditions.

pNK cells augmented with CXCR1 or CXCR2 exhibited enhanced chemoattractive capacity

To assess the chemoattractive ability of pNK cells augmented with CXCR1 or CXCR2 toward pancreatic cancer cells, we assessed an *in vitro* chemotaxis using a Transwell-mediated cell migration assay (Figure 3A). To track the migration of NK cells toward pancreatic cancer cells or HPaSteC cells, each NK cell line was labeled with Vybrant DiD dye and incubated in the upper Transwell, whereas target

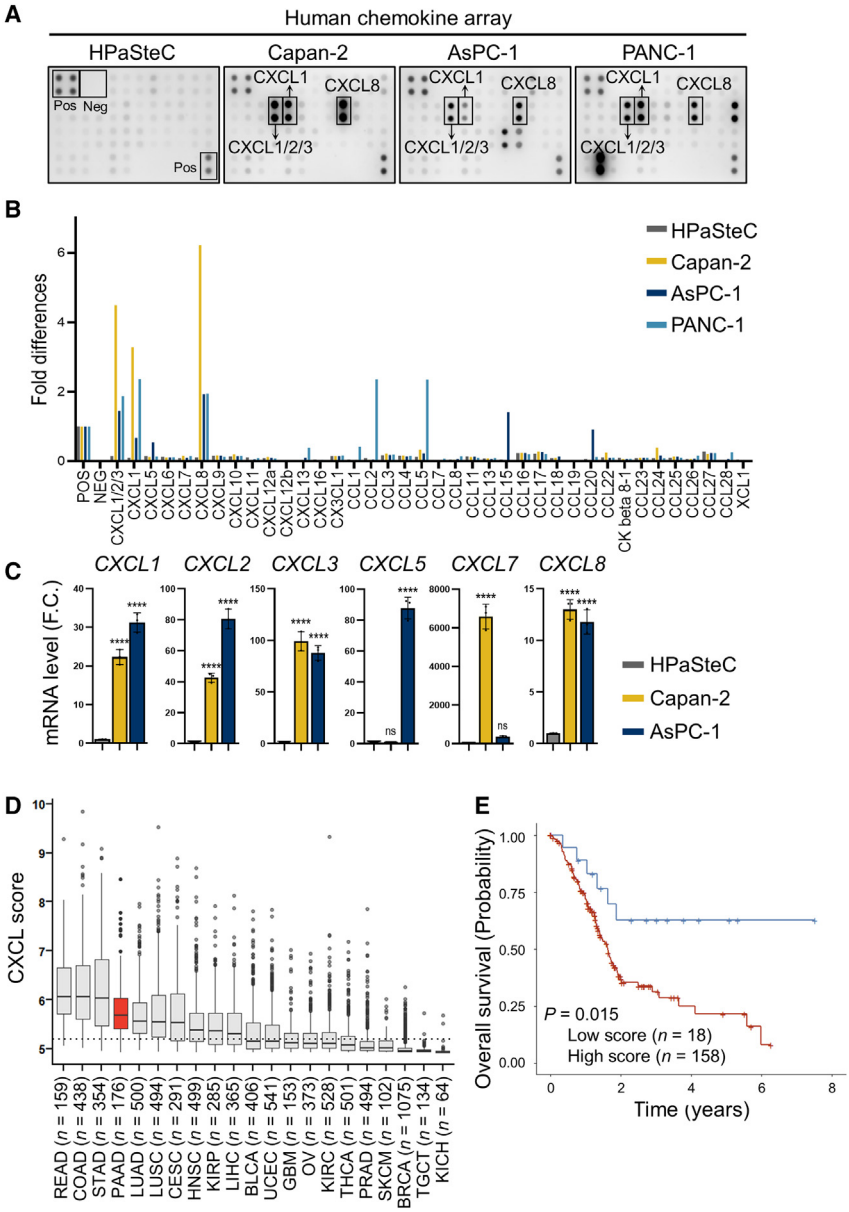

Figure 1. Profiling of chemokine ligands secreted from pancreatic cancer cells

(A and B) A human chemokine array was performed using culture supernatant from human pancreatic cancer cells, including Capan-2, AsPC-1, and PANC-1. Human primary pancreatic stellate cells (HPaSteC) were used as a negative control. (B) The expression of secreted chemokine ligands from each cell line was quantified and normalized to standard positive spots by measuring their pixel intensity using the ChemiDoc software (n = 2). (C) Relative mRNA expression of CXCR1 or CXCR2 ligands was determined using total cell extracts for each cell line. Quantitative data were obtained from three independent experiments per group (n = 3). p values were determined using a one-way ANOVA followed by a multiple comparison test; ****p < 0.0001, ns: not significant. (D) CXCL score distribution in The Cancer Genome Atlas pan-cancer cohort. Whisker-box plots were used to represent the distribution of the CXCL score, including those for CXCL1, CXCL2, CXCL3, CXCL5, CXCL6, CXCL7, and CXCL8, across different cancer types. The red color represents pancreatic adenocarcinoma. Abbreviations for cancer types are described in the materials and methods section. (E) Kaplan-Meier overall survival analysis was performed on patients with pancreatic cancer (n = 176) using high vs. low CXCL scores, with a cutoff of 5.336. p values were calculated using a standard log rank test.

cells stained with either DiO or Calcein-AM were seeded in the lower well (Figures 3B and S5). Both CXCR1- and CXCR2-augmented NK cells exhibited higher migration toward cancer cells than the mock-pNK cells, indicating an enhanced chemoattractive response. We further investigated the chemotactic ability of NK cells augmented with CXCR1 or CXCR2 toward colorectal cancers (i.e., HT-29 and SW620) with high expression of CXCL3 and/or CXCL5 (Figure S6). NK cells overexpressing either CXCR1 or CXCR2 did not exhibit increased chemoattractive responses to the colorectal cancer cells. Taken together, these findings suggest that pancreatic cancers, which secrete a broader range of CXCR1 and CXCR2 ligands, may attract migrating CXCR1/2-augmented NK cells more effectively than colon cancer cells, which secrete a limited array of CXCR2 ligands.

We then sought to confirm the role of CXCR1 and CXCR2 ligands secreted by pancreatic cancer cells in attracting CXCR1- or CXCR2-thethered NK cells (Figure 3C). To this end, we pre-treated Capan-2 cells, representative of pancreatic cancer, with navarixin[37]—a targeted CXCR1/2 antagonist—for 24 h before performing an *in vitro* chemotactic assay. Navarixin pre-treatment markedly reduced the migration of pNK cells augmented with CXCR1 or CXCR2 toward the Capan-2 cells.

pNK cells augmented with CXCR1 or CXCR2 exhibit improved *in vivo* infiltration

To investigate the *in vivo* homing effect of pNK cells augmented with CXCR1 or CXCR2 on pancreatic cancer cells, we monitored the biodistribution of DiD-labeled engineered NK cells after their intravenous injection into mice bearing subcutaneous Capan-2 pancreatic tumor xenografts (Figures 4A and 4B). *In vivo* fluorescence from DiD-labeled NK cells was visualized at different time points. CXCR1- and CXCR2-pNK cells exhibited remarkably high trafficking to the tumor sites (Figure 4B). Moreover, *ex vivo* biodistribution analysis revealed significantly stronger infiltration of CXCR2-pNK cells than CXCR1-pNK cells 48 h after administering NK cells (Figure 4C). Consistently, strong infiltration of CXCR2-pNK cells was observed in the excised tumor sections (Figure 4D). We further verified the presence of infiltrated pNK cells throughout the live tumor tissues via flow cytometry conducted 48 h after pNK cell injection (Figures 4E and S7). Notably,

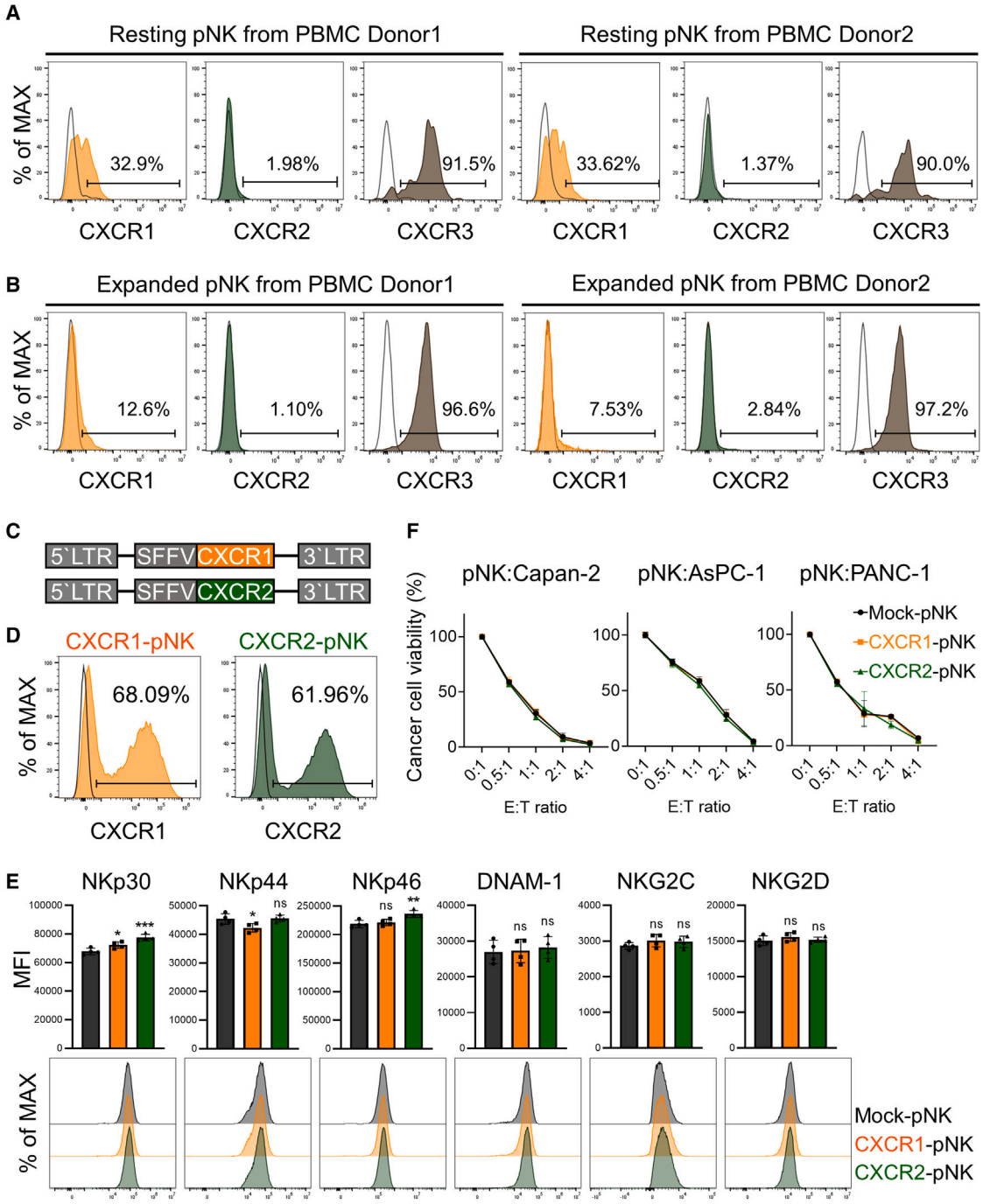

Figure 2. Generation and characterization of CXCR1/2-tethered human primary natural killer (pNK) cells

(A and B) Flow cytometry analysis of the endogenous surface expression of chemokine receptor CXCR1–3 in NK cells. Resting (A) and *ex vivo* expanded (B) pNK cells were obtained from peripheral blood mononuclear cells (PBMCs) of two different healthy donors. (C) Lentiviral constructs of CXCR1 and CXCR2 were used for overexpression. (D) Expanded pNK cells were transduced with lentivirus carrying the CXCR1 or CXCR2 constructs to generate CXCR1-overexpressing (CXCR1-pNK) or CXCR2-overexpressing (CXCR2-pNK) pNK cells, respectively. The transduction efficacy was analyzed using flow cytometry. (E) Flow cytometry analysis of the expression of activating receptors on engineered pNK cells. Quantitative data were obtained from three independent experiments per group (n = 3). p values were determined using one-way ANOVA followed by a multiple comparison test; *p < 0.05, **p < 0.01, ***p < 0.001, ns: not significant. (F) Evaluation of cancer-killing efficacy of engineered pNK cells toward pancreatic cancer cells at indicated effector-to-target (E:T) ratios. Cancer cell viability was assessed by measuring the luciferase activity.

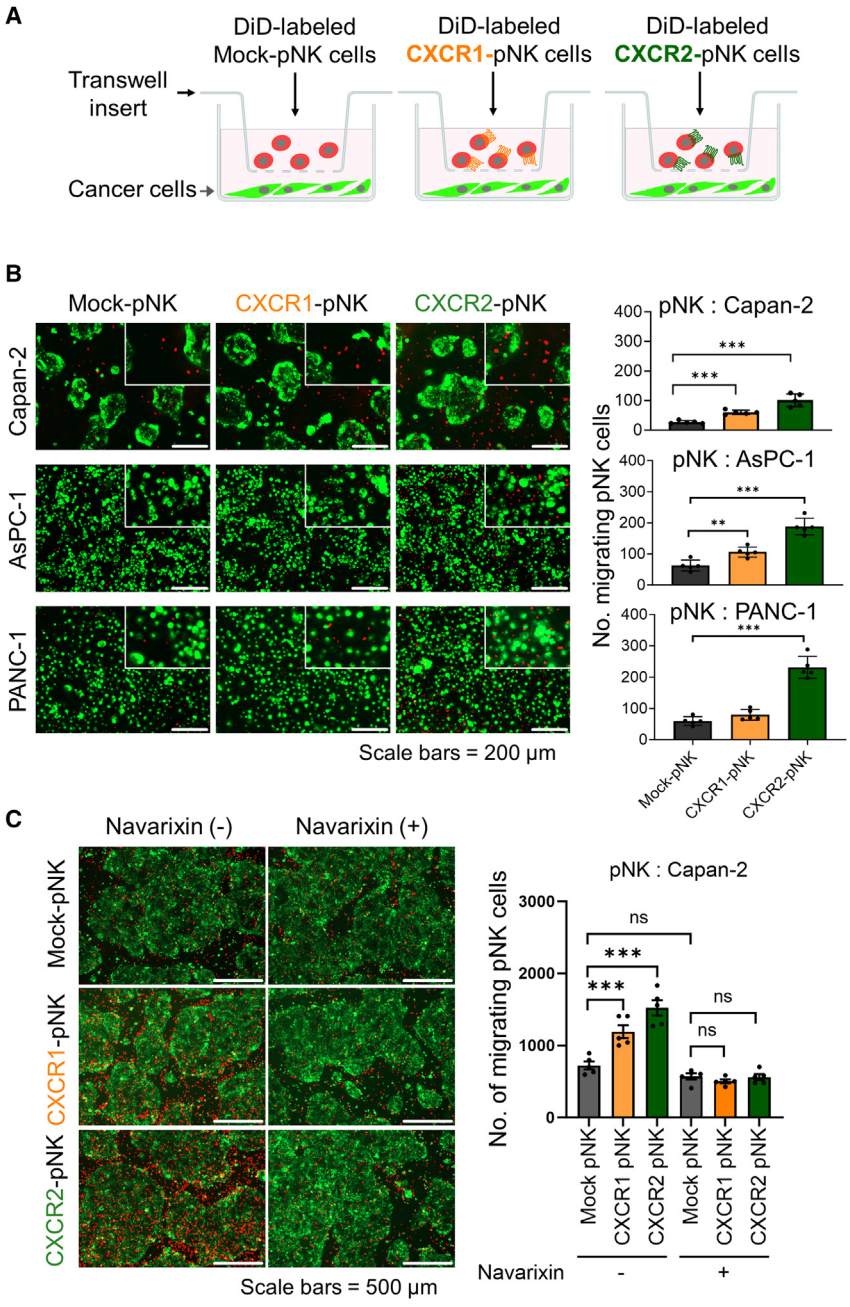

Figure 3. Enhanced migration of human primary natural killer (pNK) cells overexpressing CXCR1 or CXCR2 toward pancreatic cancer cells

(A) Schematic illustration of the Transwell-mediated chemotaxis assay designed to evaluate the migration of CXCR1-and CXCR2-overexpressing pNK cells. (B) For visualization of each cancer cell type, Vybrant DiO fluorescence dye was used to stain Capan-2, AsPC-1, and PANC-1 cells. Vybrant DiD-labeled pNK cells were subsequently added to the Transwell insert. Fluorescence images were captured from the bottom of the lower well 30 min after seeding pNK. The numbers of migrating pNK cells in the lower well were quantified via live cell imaging analysis. p-values were determined using a student's t-test; $^{**}p < 0.01$, $^{***}p < 0.001$. (C) Migration of CXCR1- and CXCR2-augmented pNK cells following pre-treatment of cancer cells with navarixin, a selective CXCR1/2 antagonist, for 24 h. Quantitative analyses were conducted with two-way ANOVA followed by a multiple comparison test; $^{***}p < 0.001$, ns: not significant. Data are represented as means ± standard error of the mean (SEM).

in the group treated with CXCR2-pNK cells, CD56-and DiD-positive pNK cells were prominently detected.

CAR-pNK cells augmented with CXCR2 exhibit enhanced infiltration and anti-cancer capacity

To enhance the anti-cancer activity of pNK cells for effective pancreatic cancer treatment, we generated cancer-directed pNK cells by incorporating a solid tumor-targeting CAR gene along with CXCR1 or CXCR2 (Figure 5A). Mesothelin (MSLN) is a tumor antigen that is overexpressed in various solid tumors, including pancreatic cancer.[38] Therefore, we combined an anti-MSLN (SS single chain variable fragment [scFv]) CAR[39] with either CXCR1 or CXCR2 in pNK cells to achieve synergistic anti-tumor activity. The transduction efficiencies of CAR-NK (SS), CXCR1-augmented CAR (SS-CXCR1), and CXCR2-augmented CAR (SS-CXCR2) pNK cells were approximately 39%–40% (Figure 5B).

Next, we assessed the *in vitro* cancer-killing efficacy of CXCR1- and CXCR2-augmented CAR-NK cells against MSLN-positive Capan-2 and MSLN-negative PANC-1 cells (Figures 5C and 5D). SS-CXCR2-pNK cells demonstrated improved cancer-killing activity against MSLN-positive Capan-2 cells (Figure 5D, left panel); however, these cells did not significantly kill MSLN-negative PANC-1 cells (Figure 5D, right panel). These findings indicated that the combination of MSLN-directed SS CAR-pNK cells with enhanced tumor infiltrating properties, achieved through CXCR2 augmentation, specifically enhanced the killing efficacy of MSLN-positive cancer cells. That is, the presence of CXCR2 facilitated the efficient migration of SS CAR-pNK cells to MSLN-positive tumor sites, leading to enhanced cancer cell killing.

Next, to investigate the potential mechanism underlying the synergistic anti-tumor activity of SS-CXCR2-pNK cells, we conducted an *in vitro* chemotaxis assay to assess their migratory behavior in the presence of Capan2 cells (Figure 5E). Real-time fluorescence images were obtained at various time points up to 12 h after adding Hoechst-labeled pNK cells to a Transwell system. SS-CXCR2-pNK

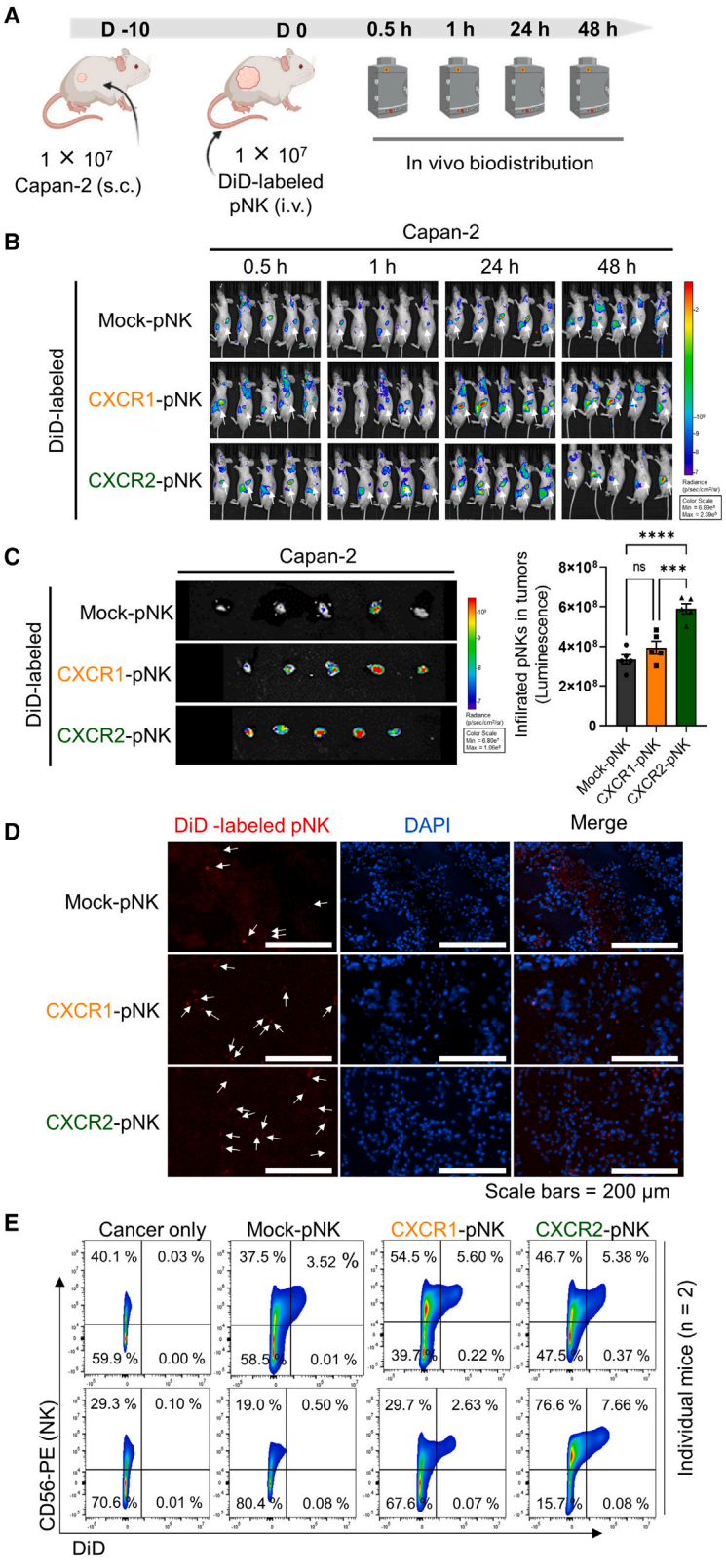

Figure 4. Biodistribution of human primary natural killer (pNK) cells augmented with CXCR1 or CXCR2 in Capan-2-bearing xenograft mice

(A) Experimental design scheme of the *in vivo* biodistribution analysis of engineered pNK cells. Vybrant DiD-labeled pNK cells were intravenously injected into Capan-2-bearing subcutaneous xenograft mice. (B) Visualization of the targeting of DiD-labeled pNK cells to Capan-2 tumor sites at the indicated time points using the IVIS system. Arrows indicate the subcutaneously injected tumors. (C) Visualization of infiltrated pNK cells in excised tumors 48 h after pNK cell injection, with *ex vivo* fluorescence imaging using the IVIS system. Quantification of infiltrated pNK cells. Data represent the means ± standard error of the mean (SEM). ***$p < 0.001$, ****$p < 0.0001$, ns: not significant; a one-way ANOVA with a multiple comparison test was used. (D) Tumor sections were stained with DAPI for counterstaining. Arrows indicate DiD-labeled pNK cells. (E) Proportion of live infiltrating pNK cells from the total tumor tissues of two individual mice, assessed by flow cytometry. CD56 and DiD-positive NK cells were quantified 48 h post-NK cell injection.

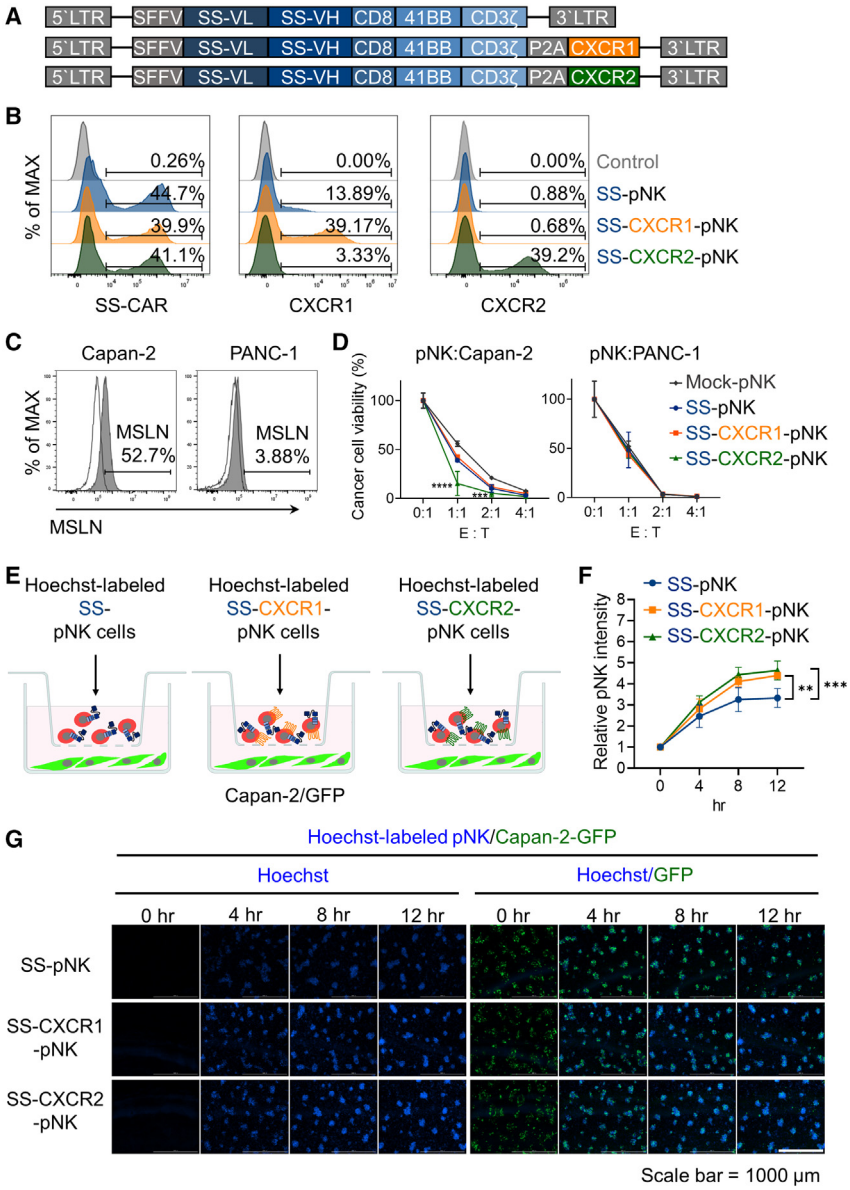

Figure 5. Amplified anti-cancer activity of CXCR2-augmenting anti-MSLN CAR-NK toward mesothelin (MSLN)-positive cancer with enhanced infiltration

(A and B) The generation of a second-generation CAR gene containing SS scFv, which targets MSLN, augmented with CXCR1 or CXCR2 in human primary natural killer (pNK) cells. (B) Flow cytometry analysis of transduction efficiency of engineered CAR-NK. (C) Flow cytometry analysis of the surface expression of MSLN on pancreatic cancer cells, including Capan-2 and PANC-1. Capan-2 shows strong expression of MSLN, whereas PANC-1 shows weak expression. (D) *In vitro* cancer cell-killing efficacy of CAR-NK combined with CXCR1 or CXCR2. Engineered CAR-NK cells were co-incubated with luciferase-overexpressing cancer cells of each type at the indicated E:T ratios for 24 h, and then luminescence signals from live cancer cells were quantified. p values were determined using a two-way ANOVA followed by a multiple comparison test for data from triplicate of each group; ***$p < 0.001$, ****$p < 0.0001$. (E–G) Chemotaxis assay of CXCR1-or CXCR2-tethered CAR-NK cells toward Capan-2 cells. (E) Schematic representation of the chemotaxis assay. Each NK cell was stained with Hoechst, whereas Capan-2 cells stably expressed GFP. (F) Quantification of infiltrated CAR-NK cells, measured every 4 h up to 12 h after adding NK cells in the Transwell, as analyzed using a live cell imaging system. p-values were determined using a two-way ANOVA followed by a multiple comparison test for data from triplicate of each group; **$p < 0.01$, ***$p < 0.001$. (G) Representative images showing the chemoattractive movement of pNK cells toward GFP-expressing Capan-2 at the indicated time points.

cells exhibited significant infiltration toward Capan2 cells compared with other NK cells (Figures 5F and 5G).

Tumor-mimetic organoid-based killing of CAR-pNK cells augmented with CXCR2

To investigate the synergistic effects of CXCR2-tethered CAR-pNK cells in a more clinically relevant setting, we evaluated their anti-tumor activity against organoids derived from patients with pancreatic cancer that closely resemble tumor tissues (Figures 6A, 6B, and S8). Three different pNK cell populations, SS-pNK, SS-CXCR1-pNK, and SS-CXCR2-pNK, were co-cultured with SNU-2571-CO and SNU-213-CO patient-derived organoids, which notably secrete or express high levels of CXCR1 and CXCR2 ligands (Figures 6C, 6D, S1, and S8). Subsequently, we assessed NK-mediated killing of the organoids by detecting the fluorescence emitted from the dTomato-expressing organoids (Figures 6E, 6F, and S8). Calcein-AM-labeled NK cells were used to visualize NK cell infiltration (Figures 6G and S8F). Consistent with our *in vitro* killing assay data, SS-CXCR2-NK cells exhibited significantly enhanced organoid-killing efficacy compared with SS-pNK or SS-CXCR2-pNK cells. However, SS-CXCR1-pNK cells did not exhibit any additive or synergistic killing effects compared with SS-NK cells with MSLN-dependent organoid-killing abilities. In summary, the observed improvement in the anti-tumor activity of SS-CXCR2-NK cells highlight their potential as a clinically relevant modality for the effective treatment of pancreatic cancer. The enhanced infiltration and tumor-killing capabilities of these engineered NK cells offer promising prospects for improving the therapeutic outcomes in patients with pancreatic cancer (Figure 7).

DISCUSSION

The TME in pancreatic cancer is characterized by a dense and restrictive architecture that hampers the infiltration of cytotoxic immune cells, leading to limited anti-tumor immune responses to CAR

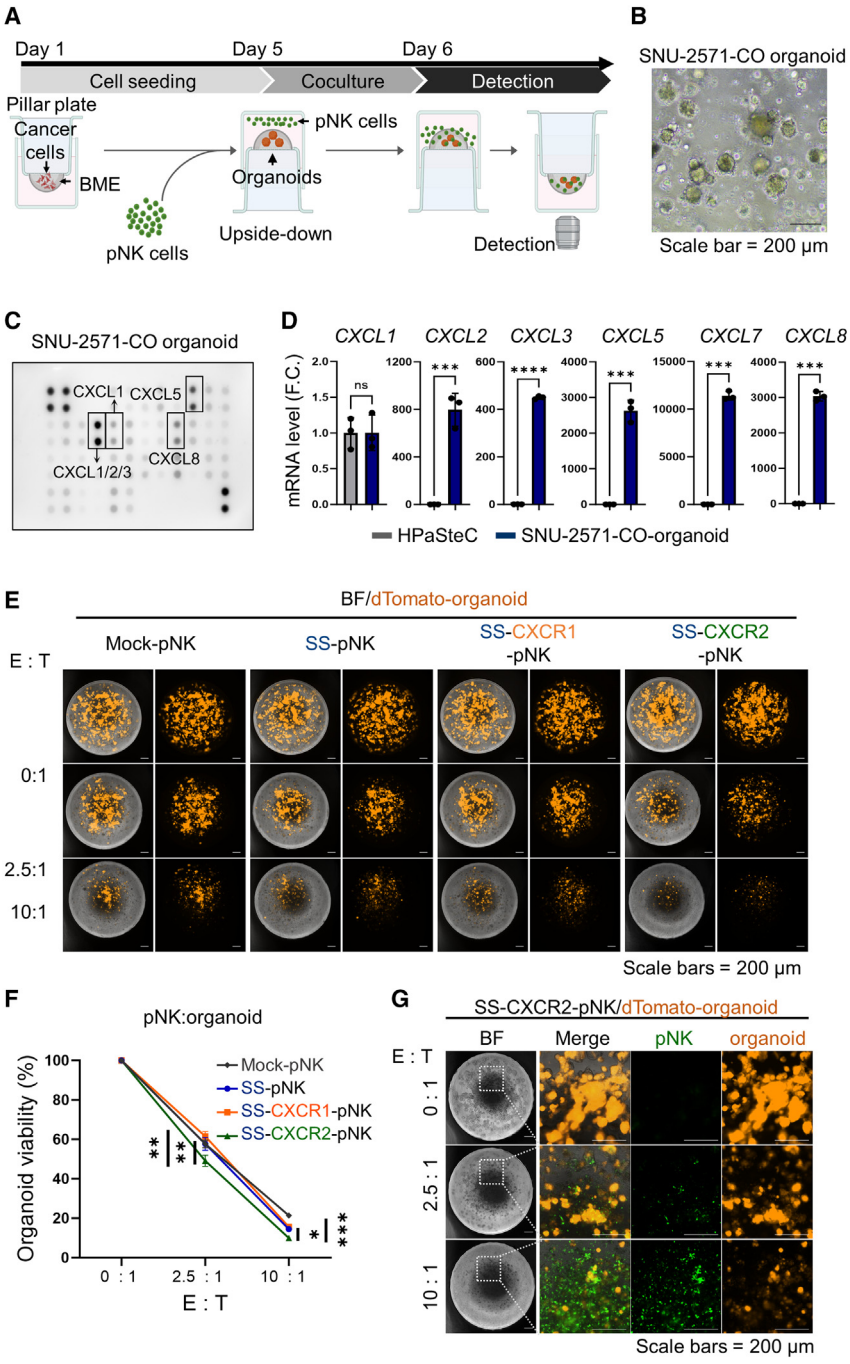

Figure 6. Human primary natural killer (pNK) cell-mediated killing of patient-derived organoids

(A) Schematic illustration of pNK-organoid co-culture. The 3D organoids and pNK cells were co-cultured using a micro-pillar system, and the viability of dTomato-overexpressing organoids was assessed. (B) Representative brightfield images of patient-derived pancreatic cancer organoid lines, SNU-2571-CO. (C) Human chemokine array analysis of total lysates from SNU-2571-CO organoids. (D) Relative mRNA expression of CXCR1 or CXCR2 ligands from total organoid extracts. p values were determined using a Student's t test; ***$p < 0.001$, ****$p < 0.0001$, ns: not significant. (E and F) pNK-mediated killing of patient-derived organoids. (E) Representative fluorescence images of dTomato-expressing SNU-2571-CO organoids co-cultured with each group of pNK cells at the indicated effector (NK cells) vs. target (organoids) ratios. (F) Relative viability of organoids analyzed using mean fluorescence intensity (MFI) and normalized to the MFI of the organoid-only group. The graph represents the mean ± SEM of data from quadruplets of each group. p values were determined using a two-way ANOVA followed by a multiple comparison test; *$p < 0.05$, **$p < 0.01$, ***$p < 0.001$. (G) Representative images showing pNK cells infiltrated into organoids at the indicated E:T ratios; brightfield (BF) images of the cancer organoids (orange) and infiltrated NK cells (green).

therapies.[40] Thus, the effective homing of CAR-engineered immune cells to tumor sites is crucial for achieving clinical therapeutic benefits against pancreatic cancer. To overcome the challenge of low CAR-T/NK cell infiltrations, the chemokine system has been explored to provide key migratory signals.[41] Various strategies have been developed to harness specific chemokine-chemokine receptor axes, particularly for NK-mediated immunotherapy. One approach involves *ex vivo* NK cell expansion methods using different feeder systems and media conditions, which create NK cell populations with distinct chemokine receptor expression patterns. For instance, IL-2 or IL-15 stimulation significantly upregulates the expression of CXCR3 in NK cells, promoting their migration toward CXCL10-producing tumor sites.[19,42] Moreover, the addition of glucocorticoids in the presence of IL-15 can further enhance CXCR3 expression in NK cells.[43] Although cytotoxic $CD56^{dim}$ NK cells—the main subpopulation in the blood—lack CCR7, priming $CD56^{dim}$ NK cells with IL-18 induces the acquisition of lymph node-homing properties through increased CCR7 expression.[44] Notably, the expression of chemokine receptors can be modulated through trogocytosis—a contact contact-dependent process involving the transfer of membrane fragments from donor to recipient cells. Co-culturing NK cells with irradiated CCR7-expressing K562 cells as donor cells leads to transient but high expression of CCR7 in NK cells.[30] Although these strategies are rapid and effective for clinical-scale manufacturing processes, their effects are often transient and difficult to sustain. Meanwhile, genetically engineered NK cells that directly overexpress specific chemokine receptors offer a promising approach to address the risk of receptor loss. This strategy enables NK cells to exhibit persistent and stable expression of desired chemokine receptors, facilitating enhanced tumor homing and

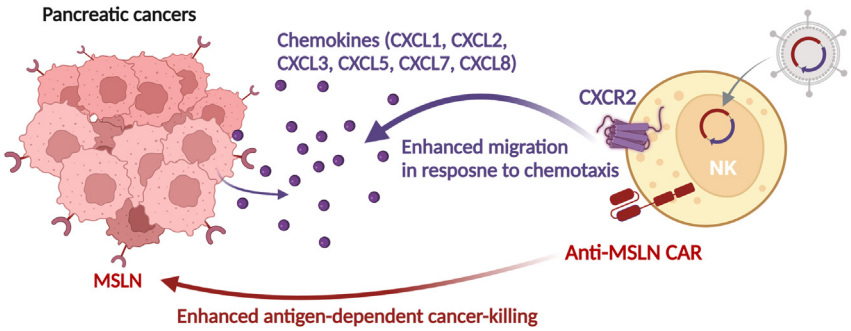

Figure 7. Working mechanism of anti-MSLN chimeric antigen receptor (CAR)-engineered natural killer (CAR-NK) cells augmented with CXCR2

Pancreatic cancers exhibit strong secretion of CXCR1 and CXCR2 ligands, such as CXCL1, CXCL2, CXCL3, CXCL5, CXCL7, and CXCL8. Anti-MSLN CAR-pNK cells were genetically augmented with CXCR1 or CXCR2. CXCR2-tethered CAR-NK cells exhibit synergistic anti-tumor activity against MSLN-positive pancreatic cancer cells, accompanied by enhanced NK cell infiltration within *in vitro* 2D co-cultures and 3D tumor microenvironment (TME)-mimicking patient-derived model.

infiltration. In conclusion, the complex TME of pancreatic cancer poses challenges, including limited immune cell infiltration, for effective immunotherapy. Harnessing the chemokine system, by modulating chemokine receptor expression or direct genetic engineering, has considerable potential to enhance the homing and infiltration of CAR-engineered cells, such as NK cells, and to improve the efficacy of immunotherapeutic approaches for pancreatic cancers.

In this study, we observed robust secretion of CXCR1 and CXCR2 ligands, including CXCL1, CXCL2, CXCL3, CXCL5, CXCL7, and CXCL8, in pancreatic cancers. Accordingly, we sought to improve the infiltration and cytotoxicity of anti-MSLN CAR-NK cells in pancreatic cancer by augmenting their expression of CXCR1 and CXCR2. Using *in vitro* 2D co-culture and 3D TME-relevant organoid models, we evaluated the activity of engineered CAR-NK cells against MSLN-positive cancers. Only CXCR2-augmented anti-MSLN CAR-NK cells, not CXCR1-augmented CAR-NK cells, demonstrated significantly improved killing efficacy against MSLN-positive cancers. Despite the strong secretion of CXCR1 ligands in pancreatic cancers, enhanced killing efficacy was not observed in CXCR1-augmented CAR-NK cells. This discrepancy could be explained by the limited availability of ligands for CXCR1, i.e., CXCL1 and CXCL8, compared with the multiple ligands (CXCL1, CXCL2, CXCL3, CXCL5, CXCL6, CXCL7, and CXCL8) for CXCR2. Therefore, CAR-NK cells augmented solely with CXCR2 exhibited a more effective cancer treating effect with enhanced infiltration against pancreatic cancer. These findings highlight the importance of selecting appropriate chemokine receptors for CAR-NK cell augmentation to achieve optimal therapeutic outcomes in pancreatic cancer. The selective augmentation of CXCR2 with multiple ligands appears to be more effective in improving the activity and infiltration of CAR-NK cells. Further studies are required to better characterize the underlying mechanisms and to optimize the CXCR2-augmented CAR-NK approach for effective treatment of pancreatic cancer.

Herein, we aimed to enhance the therapeutic efficacy of MSLN-targeting CAR-engineered NK cells against pancreatic cancers by improving their tumor-homing capabilities (Figure 7). We identified CXCR1 and CXCR2 ligands as potential mediators for guiding CAR-NK cells to tumor sites based on the chemokine ligand profile of pancreatic cancer cells. By incorporating CXCR2 into CAR-NK cells, we observed enhanced tumor killing and increased infiltration into tumor sites in 2D and 3D organoid models. Our findings highlight the potential of CXCR2-augmented CAR-NK cells as a clinically relevant modality for the effective treatment of pancreatic cancer.

MATERIALS AND METHODS

Cell cultures

HPaSteCs were obtained from ScienCell Research Laboratories (Carlsbad, CA, USA). The pancreatic cancer cell lines, PANC-1, Capan-2, and AsPC-1, were acquired from the Korean Cell Line Bank (KCLB, Seoul, Korea). HPaSteC and PANC-1 cells were cultured in Dulbecco's modified Eagle's medium (DMEM; Welgene, Daegu, Korea) supplemented with 10% fetal bovine serum (FBS; Welgene) and 1% antibiotic-antimycotic solution (Welgene). Capan-2 and AsPC-1 cells were maintained in RPMI-1640 medium (Welgene) supplemented with 10% FBS (Welgene) and 1% antibiotic-antimycotic solution (Welgene). The human colorectal adenocarcinoma cell lines, HT-29 and SW620, were obtained from the KCLB. Both HT-29 and SW620 cells were cultured in RPMI 1640 medium (Welgene) supplemented with 10% FBS (Welgene) and 1% antibiotic-antimycotic solution (Welgene).

Isolation and *ex vivo* expansion of human pNK cells

PBMCs were purchased from Lonza (Morristown, NJ, USA). NK MACS (Miltenyl Biotec, Bergisch Gladbach, Germany) medium was used for cell culture. Primary NK (pNK) cells were expanded and maintained in the presence of IL-2 (200 IU/mL) and IL-15 (10 ng/mL; PeproTech, Cranbury, NJ, USA), and co-cultured with K562 feeder cells obtained from ATCC (Manassas, VA, USA). Following 2 weeks of expansion, pNK cells were isolated using an NK cell isolation kit (Miltenyi Biotec) according to the manufacturer's instructions.

Human chemokine array

The following experimental procedure was performed to assess the levels of human chemokines in HPaSteC, Capan-2, AsPC-1, and PANC-1 cells. Each cell type was cultured in serum-free growth medium for 24 h. Subsequently, cell culture media from each cell type were collected and analyzed for human chemokine levels using the human chemokine antibody array C1 (Raybiotech, Atlanta, GA, USA). Membranes containing chemokines were detected using the

ChemiDoc system (Bio-Rad, Hercules, CA, USA). For quantitating chemokine levels in patient-derived organoids, the SNU-213-CO cell pellets were lysed, and the lysate was analyzed with the human chemokine antibody array C1 (Raybiotech).

Quantitative reverse-transcription PCR (qRT-PCR) analysis

Total RNA was extracted from each cell line using a RNeasy Mini Kit (74104; QIAGEN, Hilden, Germany); cDNA was synthesized using the iScript cDNA Synthesis Kit (1708891; Bio-Rad) following the manufacturer's protocol. qRT-PCR was conducted on a QuantStudio 1 Real-Time PCR System (Applied Biosystems, Foster City, CA, USA) using FastStart Universal SYBR Green Master (04913850001; Roche, Mannheim, Germany). Specific target primers were used to obtain amplicons for qRT-PCR analysis (Table S1).

Calculation of CXCL scores

The expression score of seven CXCL genes, namely *CXCL1*, *CXCL2*, *CXCL3*, *CXCL5*, *CXCL6*, *CXCL7*, and *CXCL8*, were analyzed in a pan-cancer context using data from TCGA pan-cancer cohort consisting of 21 cancer types (n = 7932). The mRNA expression data were downloaded from https://portal.gdc.cancer.gov/ in the available fragments per kilobase per million mapped fragments (FPKM) format. The FPKM value of each gene was transformed using the *Z* score, z = (x − mean value)/standard deviation, across all samples, followed by further transformation using the t score, t = 10z + 50. The CXCL score was calculated for each sample using the following formula: log2(∑t-scores of seven genes +1). Each abbreviation in Figure 1D corresponds to a specific cancer type as follows: BLCA, bladder urothelial carcinoma; BRCA, breast invasive carcinoma; CESC, cervical squamous cell carcinoma and endocervical adenocarcinoma; COAD, colon adenocarcinoma; GBM, glioblastoma multiforme; HNSC, head and neck squamous cell carcinoma; KICH, kidney chromophobe; KIRC, kidney renal clear cell carcinoma; KIRP, kidney renal papillary cell carcinoma; LIHC, liver hepatocellular carcinoma; LUAD, lung adenocarcinoma; LUSC, lung squamous cell carcinoma; OV, ovarian serous cystadenocarcinoma; PAAD, pancreatic adenocarcinoma; PRAD, prostate adenocarcinoma; READ, rectum adenocarcinoma; SKCM, skin cutaneous melanoma; STAD, stomach adenocarcinoma; TGCT, testicular germ cell tumors; THCA, thyroid carcinoma; UCEC, uterine corpus endometrial carcinoma.

Survival analysis

To analyze the overall survival of pan-cancer patients, the overall survival data were obtained from https://portal.gdc.cancer.gov/. Specifically, the Kaplan-Meier survival analysis was performed on patients with pancreatic cancer (n = 176) based on their CXCL scores. The survival analysis was conducted using the R "survival" package. The optimal cutoff was obtained using the R "maxstat" package. Statistical significance was analyzed using the standard log rank test.

Western blot analysis

Cells were lysed using RIPA buffer (ThermoFisher Scientific, Waltham, MA, USA) supplemented with a protein inhibitor cocktail. The lysates were incubated on ice for 20 min and collected by centrifugation at 14,000 rpm for 20 min. Proteins in the total lysates were separated using SDS-PAGE and transferred onto a polyvinylidene difluoride membrane. The membranes were blocked with 5% skim milk in 0.2% Tween 20/TBS and subsequently incubated with a primary antibody, followed by a secondary antibody. The proteins were visualized using the ChemiDoc system (Bio-Rad). The following antibodies were used: anti-CXCL1/CXCL2 antibody (24376; Cell Signaling Technology [CST], Danvers, MA, USA) and anti-rabbit immunoglobulin (Ig)G and HRP-linked antibody (7074; CST).

Luminescence-based cancer-killing assay

To evaluate NK-mediated cancer killing, cancer cells were genetically engineered to overexpress NanoLuc luciferase, as described previously.[45] Cancer cells expressing NanoLuc luciferase were then co-cultured with genetically engineered pNK cells at designated effector: target (E:T) ratios for 24 h. Following the co-culture period, luminescence signals were measured using the Nano-Glo luciferase assay system (N1120; Promega, Madison, WI, USA) in accordance with the manufacturer's instructions. This assay system allows the quantification of luciferase activity and serves as an indicator of NK cell-mediated cancer cell death.

Generation of genetically engineered pNK cells

To construct the CAR plasmid for overexpressing chemokine receptors, DNA fragments encoding a second-generation CAR containing the SS scFv (US Patent: US7081518; https://patents.google.com/patent/US7081518?oq=patent:7081518) and either CXCR1 or CXCR2 were synthesized by Cosmo Genetech (Seoul, Korea). These DNA fragments were incorporated into the pCDH lentivirus vector (72266; Addgene, Cambridge, MA, USA) using the NEBuilder HiFi DNA assembly kit (New England Biolabs, Ipswich, MA, USA).

To generate chemokine receptor-overexpressing CAR-NK cells, lentiviruses carrying SS CAR, SS CAR-CXCR1, and SS CAR-CXCR2 constructs were produced. For lentivirus production, HEK293T cells were seeded at a density of 2×10^6 cells in 100-mm dishes 24 h prior to transfection. The shuttle vector, psPAX2 packaging vector, and baboon envelope vector were transfected into the cells using PEI transfection reagent as described previously.[45] Lentivirus-containing media were collected 24 and 48 h post-transfection. The harvested viruses were filtered through a 0.45-μm filter (Minisart 16533-K; Sartorius, Göttingen, Germany) and subsequently concentrated using the Lenti-X concentrator (631232; Takara, Tokyo, Japan).

For transduction, pNK cells were first treated with IL-12 (10 ng/mL), IL-15 (50 ng/mL), and IL-18 (50 ng/mL) 24 h prior to transduction. Subsequently, 2×10^6 cells were mixed with lentivirus at a multiplicity of infection (MOI) of 10, along with Vectofusin-1 (10 μg/mL) (130-111-163; Miltenyi Biotec) to enhance the transduction efficiency. The transduction efficiency was evaluated using flow cytometry with APC anti-human CD181 (CXCR1) antibody (320612; BioLegend, San Diego, CA, USA) and APC anti-human CD182 (CXCR2) antibody (320710; BioLegend) to detect CXCR1 and

CXCR2 expression in transduced NK cells. Furthermore, the expression of anti-mesothelin (MSLN; SS scFv)[46] CAR was assessed using biotinylated human MSLN recombinant proteins and PE-conjugated streptavidin (554061; BD Pharmingen, San Diego, CA, USA).

Live cell imaging-based chemotaxis assay

For the *in vitro* chemotaxis assay, Vybrant DiO- (V22886; ThermoFisher Scientific) labeled cancer cells were seeded at a density of 0.2×10^6 cells per well in a 24-well plate. Subsequently Vybrant DiD- (V22887; ThermoFisher Scientific) labeled pNK cells were added to the 6.5-mm Transwell insert at a density of 0.5×10^6 cells (3422; Costar, Cambridge, MA, USA). To monitor the chemotaxis process in real time, the cells were maintained under a humidified atmosphere containing 5% CO_2 at 37°C, and fluorescence images were captured 30 min after the co-culture of pNK cells using BioTek Lionheart FX automated live cell imager (Agilent, Technologies, Santa Clare, CA, USA). To quantify the chemotactic attraction of pNK cells, the images were analyzed using the Gen5 software (Agilent, Technologies, Santa Clare, CA, USA). The software allowed for the calculation and analysis of the migrated pNK cells toward cancer cells at specific time points.

To evaluate the effect of navarixin (8506; Selleck Chemicals, Houston, TX, USA)—a CXCR1/2 inhibitor—on the chemotactic ability of pNK cells toward Vybrant DiO-labeled Capan-2 cells, Capan-2 cells (0.5×10^6 cells) were pre-treated with 50 μM navarixin for 24 h prior to the chemotaxis assay. Following this, Vybrant DiD-labeled pNK cells were added to the 6.5-mm Transwell insert at a density of 0.5×10^6 cells to conduct the chemotaxis assay as described previously.

To test the chemotaxis-mediated cancer cell killing and infiltration by CXCR1- and CXCR2-augmented CAR-NK cells, GFP-expressing cancer cells were seeded at a density of 0.2×10^6 cells per well in a 24-well plate. Hoechst-labeled (62249; ThermoFisher Scientific) pNK cells were then added to the 6.5-mm Transwell insert at a density of 0.5×10^6 cells. Fluorescence images were captured 0, 4, 8, and 24 h after initiating co-culture with the pNK cells. All images were taken at these specific time points using the BioTek Lionheart FX automated live cell imager (Agilent Technologies).

Flow cytometry

Flow cytometric analysis was performed using CytoFLEX (Beckman Coulter Life Sciences, Brea, CA, USA). The FlowJo software (BD Biosciences, San Jose, CA, USA) was used for cytometric data analysis. The antibodies used were as follows: PE/Cyanine7 anti-human CD337 (NKp30) (325214; BioLegend), APC anti-human CD336 (NKp44) (325110; BioLegend), PE/Dazzle 594 anti-human CD335 (NKp46) (331930; BioLegend), Brilliant Violet 421 anti-human CD226 (DNAM-1) (338332; BioLegend), Human NKG2C/CD159c Alexa Fluor 700 (FAB138N-100; R&D Systems, Minneapolis, MN, USA), APC/Cyanine7 anti-human CD314 (NKG2D) (320824; BioLegend), PE anti-human CD56 (NCAM) (318306; BioLegend), FITC anti-human CD3 (UCHT1) (11-0038-42; eBioscience, San Diego, CA, USA), APC anti-human CD181 (CXCR1) (320612; BioLegend) and APC anti-human CD182 (CXCR2) (320710; BioLegend). Dead cells were stained with the Fixable Viability Dye eFluor 506 (65-0866-14; eBioscience).

In vivo mouse experiment

Ethical approval for the animal experiments was obtained from the Institutional Animal Care and Use Committee of KIST (KIST-2020-049), ensuring compliance with ethical guidelines and the welfare of the animal involved.

To assess the *in vivo* chemotaxis of engineered pNK cells, 9×10^6 Capan-2 cells were mixed with Matrigel (Corning, NY, USA) at a 1:1 volume ratio. The cell-Matrigel mixture was injected subcutaneously into BALB/c nude mice to establish a Capan-2-bearing mouse model. After 10 days of being administered cancer cells, each engineered pNK cell was labeled with DiD at a density of 1×10^7 cells. The labeled pNK cells were intravenously injected into the tail vein of mice. The biodistribution of pNK cells was visualized using the IVIS Spectrum Imaging System (PerkinElmer, Waltham, MA, USA) 0.5, 1, 24, and 48 h after pNK cell injection. The imaging system allowed visualization and quantification of the distribution and accumulation of labeled pNK cells within mice. Following the completion of the *in vivo* imaging studies, mice were euthanized 48 h after pNK cell injection. Capan-2 tumors were harvested for *ex vivo* distribution analyses.

To verify the infiltrated pNK cells within tumor tissues, the entire live tumor tissue from two individual mice was harvested and dissociated 48 h post-injection of DiD-labeled pNK cells. This process utilized a tumor dissociation kit (130-095-929, Miltenyi Biotec) and GentleMACS Dissociator (130-093-235, Miltenyi Biotec), following the manufacturer's instructions. The digested samples were filtered through a Falcon 40-μm Cell Strainer (352340, Corning, NY, USA). Subsequent flow cytometric analysis was performed using the PE anti-human CD56 (NCAM) antibody (318306; BioLegend) and the Fixable Viability Dye eFluor 780 (65-0865-14; eBioscience) for precise identification and viability assessment.

Patient-derived organoid culture and preparation of fluorescence-expressing cells

The pancreatic cancer organoid line SNU-213-CO was purchased from KCLB. These cells were embedded in a CultrexBME (3533-005-02; Bio-Techne, USA) dome and cultured in KCLB organoid medium. The KCLB organoid medium comprised 40% (vol/vol) Advanced DMEM/F-12 (12634028; ThermoFisher Scientific), 50% (vol/vol) L-WRN conditioned medium, 1X B27 (17504-044; ThermoFisher Scientific), 5 ng/mL hEGF (AF-100-15; PeproTech), 10 mM nicotinamide (N0636; Sigma-Aldrich, St. Louis, MO, USA), 1.25 mM N-acetyl-L-cysteine (A9165; Sigma-Aldrich), 500 nM A83-01 (29-391-0; Tocris Bioscience, Emeryville, CA, USA) and 1% penicillin/streptomycin (15140122; ThermoFisher Scientific). A lentiviral plasmid carrying a dTomato was used to establish stable fluorescence-expressing cells.

Co-culture of organoids and pNK cells and detection of cell viability

To initiate the co-culture of organoids and pNK cells, organoids were first digested into single cells and mixed with 70% basement membrane extract to achieve a final cell concentration of 1×10^6 cells/mL. The mixture (500 cells/0.5 μL per well) was then carefully spotted onto a 384-well pillar plate (MBD, Cellvitro 384PM) and allowed to solidify at 37°C in a cell culture incubator. Once gelation was complete, the pillar plate was combined with a 384-well plate filled with KCLB medium and cultured for 5 days to allow the development of organoids. On the day of co-culture, each engineered NK cell was added to a new 384-well plate (MBD, Cellvitro 384W) filled with the co-culture medium. The co-culture medium was prepared by mixing KCLB and pNK cell media at a 1:1 volume ratio. The pillar plate containing the spotted target cells was transferred to a plate with the NK cell-containing co-culture medium, followed by incubation for 24 h.[47] To visualize and detect infiltrated pNK cells, the cells were stained with Calcein-AM solution (C3099, ThermoFisher Scientific) prior to co-culture. Brightfield images and fluorescence signals were captured and analyzed using Image Exflurer (Live Cell Instrument) to assess cell viability and monitor the interaction between the organoids and pNK cells.

DATA AND CODE AVAILABILITY

All data associated with this study are present in the manuscript. Materials used in this study are available from the corresponding author upon reasonable request.

SUPPLEMENTAL INFORMATION

Supplemental information can be found online at https://doi.org/10.1016/j.omton.2024.200777.

ACKNOWLEDGMENTS

This work was supported by the National Research Foundation of Korea Grant funded by the Korean Government (grant number: 2020M3A9I4038662, 2023R1A2C2003387, RS-2023-00229101, and RS-2023-00208519) and by Korea Institute of Science and Technology (grant number: 2Z05790-19-037, 2E32331, and 2V09550). This research was also supported by Korea Drug Development Fund funded by Ministry of Science and ICT, Ministry of Trade, Industry, and Energy, and Ministry of Health and Welfare (RS-2022-00166088, Republic of Korea). This work was supported by the Creative-Pioneering Researchers Program in Seoul National University (SNU).

AUTHOR CONTRIBUTIONS

M.J. supervised the project. H.N.Y., J.H.Y., J.L., and M.J. designed the experiments. H.N.Y., J.H.Y., H.J.K., H.Y., M.J.C., J.C., M.S., M.K., S.O.L., and Y.J.K. conducted the experiments. All authors analyzed the data. J.H.Y., H.N.Y., H.J.K., J.L., and M.J. wrote the manuscript. All authors reviewed and edited the manuscript.

DECLARATION OF INTERESTS

The authors declare no competing interests.

REFERENCES

1. Yeo, D., Giardina, C., Saxena, P., and Rasko, J.E.J. (2022). The next wave of cellular immunotherapies in pancreatic cancer. Mol. Ther. Oncolytics *24*, 561–576. https://doi.org/10.1016/j.omto.2022.01.010.

2. Huber, M., Brehm, C.U., Gress, T.M., Buchholz, M., Alashkar Alhamwe, B., von Strandmann, E.P., Slater, E.P., Bartsch, J.W., Bauer, C., and Lauth, M. (2020). The Immune Microenvironment in Pancreatic Cancer. Int. J. Mol. Sci. *21*, 7307. https://doi.org/10.3390/ijms21197307.

3. Siegel, R.L., Miller, K.D., Wagle, N.S., and Jemal, A. (2023). Cancer statistics, 2023. CA. Cancer J. Clin. *73*, 17–48. https://doi.org/10.3322/caac.21763.

4. Conroy, T., Hammel, P., Hebbar, M., Ben Abdelghani, M., Wei, A.C., Raoul, J.L., Choné, L., Francois, E., Artru, P., Biagi, J.J., et al. (2018). FOLFIRINOX or Gemcitabine as Adjuvant Therapy for Pancreatic Cancer. N. Engl. J. Med. *379*, 2395–2406. https://doi.org/10.1056/NEJMoa1809775.

5. Ren, B., Cui, M., Yang, G., Wang, H., Feng, M., You, L., and Zhao, Y. (2018). Tumor microenvironment participates in metastasis of pancreatic cancer. Mol. Cancer *17*, 108. https://doi.org/10.1186/s12943-018-0858-1.

6. Vivier, E., Tomasello, E., Baratin, M., Walzer, T., and Ugolini, S. (2008). Functions of natural killer cells. Nat. Immunol. *9*, 503–510. https://doi.org/10.1038/ni1582.

7. Shimasaki, N., Jain, A., and Campana, D. (2020). NK cells for cancer immunotherapy. Nat. Rev. Drug Discov. *19*, 200–218. https://doi.org/10.1038/s41573-019-0052-1.

8. Goldenson, B.H., Hor, P., and Kaufman, D.S. (2022). iPSC-Derived Natural Killer Cell Therapies - Expansion and Targeting. Front. Immunol. *13*, 841107. https://doi.org/10.3389/fimmu.2022.841107.

9. Xie, G., Dong, H., Liang, Y., Ham, J.D., Rizwan, R., and Chen, J. (2020). CAR-NK cells: A promising cellular immunotherapy for cancer. EBioMedicine *59*, 102975. https://doi.org/10.1016/j.ebiom.2020.102975.

10. Rezvani, K., Rouce, R., Liu, E., and Shpall, E. (2017). Engineering Natural Killer Cells for Cancer Immunotherapy. Mol. Ther. *25*, 1769–1781. https://doi.org/10.1016/j.ymthe.2017.06.012.

11. Teng, K.Y., Mansour, A.G., Zhu, Z., Li, Z., Tian, L., Ma, S., Xu, B., Lu, T., Chen, H., Hou, D., et al. (2022). Off-the-Shelf Prostate Stem Cell Antigen-Directed Chimeric Antigen Receptor Natural Killer Cell Therapy to Treat Pancreatic Cancer. Gastroenterology *162*, 1319–1333. https://doi.org/10.1053/j.gastro.2021.12.281.

12. Liu, E., Marin, D., Banerjee, P., Macapinlac, H.A., Thompson, P., Basar, R., Nassif Kerbauy, L., Overman, B., Thall, P., Kaplan, M., et al. (2020). Use of CAR-Transduced Natural Killer Cells in CD19-Positive Lymphoid Tumors. N. Engl. J. Med. *382*, 545–553. https://doi.org/10.1056/NEJMoa1910607.

13. Kennedy, P.R., Felices, M., and Miller, J.S. (2022). Challenges to the broad application of allogeneic natural killer cell immunotherapy of cancer. Stem Cell Res. Ther. *13*, 165. https://doi.org/10.1186/s13287-022-02769-4.

14. Jun, E., Song, A.Y., Choi, J.W., Lee, H.H., Kim, M.Y., Ko, D.H., Kang, H.J., Kim, S.W., Bryceson, Y., Kim, S.C., and Kim, H.S. (2019). Progressive Impairment of NK Cell Cytotoxic Degranulation Is Associated With TGF-beta1 Deregulation and Disease Progression in Pancreatic Cancer. Front. Immunol. *10*, 1354. https://doi.org/10.3389/fimmu.2019.01354.

15. Zhang, L., Meng, Y., Feng, X., and Han, Z. (2022). CAR-NK cells for cancer immunotherapy: from bench to bedside. Biomark. Res. *10*, 12. https://doi.org/10.1186/s40364-022-00364-6.

16. Marofi, F., Rahman, H.S., Thangavelu, L., Dorofeev, A., Bayas-Morejón, F., Shirafkan, N., Shomali, N., Chartrand, M.S., Jarahian, M., Vahedi, G., et al. (2021). Renaissance of armored immune effector cells, CAR-NK cells, brings the higher hope for successful cancer therapy. Stem Cell Res. Ther. *12*, 200. https://doi.org/10.1186/s13287-021-02251-7.

17. Lee, M.Y., Robbins, Y., Sievers, C., Friedman, J., Abdul Sater, H., Clavijo, P.E., Judd, N., Tsong, E., Silvin, C., Soon-Shiong, P., et al. (2021). Chimeric antigen receptor engineered NK cellular immunotherapy overcomes the selection of T-cell escape variant cancer cells. J. Immunother. Cancer *9*, e002128. https://doi.org/10.1136/jitc-2020-002128.

18. Lee, Y.E., Ju, A., Choi, H.W., Kim, J.C., Kim, E.E., Kim, T.S., Kang, H.J., Kim, S.Y., Jang, J.Y., Ku, J.L., et al. (2020). Rationally designed redirection of natural killer cells

anchoring a cytotoxic ligand for pancreatic cancer treatment. J. Control. Release *326*, 310–323. https://doi.org/10.1016/j.jconrel.2020.07.016.

19. Yao, X., and Matosevic, S. (2021). Chemokine networks modulating natural killer cell trafficking to solid tumors. Cytokine Growth Factor Rev. *59*, 36–45. https://doi.org/10.1016/j.cytogfr.2020.12.003.

20. Ali, T.H., Pisanti, S., Ciaglia, E., Mortarini, R., Anichini, A., Garofalo, C., Tallerico, R., Santinami, M., Gulletta, E., Ietto, C., et al. (2014). Enrichment of CD56(dim)KIR + CD57 + highly cytotoxic NK cells in tumour-infiltrated lymph nodes of melanoma patients. Nat. Commun. *5*, 5639. https://doi.org/10.1038/ncomms6639.

21. Rocca, Y.S., Roberti, M.P., Arriaga, J.M., Amat, M., Bruno, L., Pampena, M.B., Huertas, E., Loria, F.S., Pairola, A., Bianchini, M., et al. (2013). Altered phenotype in peripheral blood and tumor-associated NK cells from colorectal cancer patients. Innate Immun. *19*, 76–85. https://doi.org/10.1177/1753425912453187.

22. Carrega, P., Morandi, B., Costa, R., Frumento, G., Forte, G., Altavilla, G., Ratto, G.B., Mingari, M.C., Moretta, L., and Ferlazzo, G. (2008). Natural killer cells infiltrating human nonsmall-cell lung cancer are enriched in CD56 bright CD16(-) cells and display an impaired capability to kill tumor cells. Cancer *112*, 863–875. https://doi.org/10.1002/cncr.23239.

23. Ran, G.H., Lin, Y.Q., Tian, L., Zhang, T., Yan, D.M., Yu, J.H., and Deng, Y.C. (2022). Natural killer cell homing and trafficking in tissues and tumors: from biology to application. Signal Transduct. Target. Ther. *7*, 205. https://doi.org/10.1038/s41392-022-01058-z.

24. Hoshikawa, M., Aoki, T., Matsushita, H., Karasaki, T., Hosoi, A., Odaira, K., Fujieda, N., Kobayashi, Y., Kambara, K., Ohara, O., et al. (2018). NK cell and IFN signatures are positive prognostic biomarkers for resectable pancreatic cancer. Biochem. Biophys. Res. Commun. *495*, 2058–2065. https://doi.org/10.1016/j.bbrc.2017.12.083.

25. Rossi, D., and Zlotnik, A. (2000). The biology of chemokines and their receptors. Annu. Rev. Immunol. *18*, 217–242. https://doi.org/10.1146/annurev.immunol.18.1.217.

26. Hughes, C.E., and Nibbs, R.J.B. (2018). A guide to chemokines and their receptors. FEBS J. *285*, 2944–2971. https://doi.org/10.1111/febs.14466.

27. Nagarsheth, N., Wicha, M.S., and Zou, W. (2017). Chemokines in the cancer microenvironment and their relevance in cancer immunotherapy. Nat. Rev. Immunol. *17*, 559–572. https://doi.org/10.1038/nri.2017.49.

28. Li, F., Sheng, Y., Hou, W., Sampath, P., Byrd, D., Thorne, S., and Zhang, Y. (2020). CCL5-armed oncolytic virus augments CCR5-engineered NK cell infiltration and antitumor efficiency. J. Immunother. Cancer *8*, e000131. https://doi.org/10.1136/jitc-2019-000131.

29. Carlsten, M., Levy, E., Karambelkar, A., Li, L., Reger, R., Berg, M., Peshwa, M.V., and Childs, R.W. (2016). Efficient mRNA-Based Genetic Engineering of Human NK Cells with High-Affinity CD16 and CCR7 Augments Rituximab-Induced ADCC against Lymphoma and Targets NK Cell Migration toward the Lymph Node-Associated Chemokine CCL19. Front. Immunol. *7*, 105. https://doi.org/10.3389/fimmu.2016.00105.

30. Somanchi, S.S., Somanchi, A., Cooper, L.J.N., and Lee, D.A. (2012). Engineering lymph node homing of ex vivo-expanded human natural killer cells via trogocytosis of the chemokine receptor CCR7. Blood *119*, 5164–5172. https://doi.org/10.1182/blood-2011-11-389924.

31. Ng, Y.Y., Tay, J.C.K., and Wang, S. (2020). CXCR1 Expression to Improve Anti-Cancer Efficacy of Intravenously Injected CAR-NK Cells in Mice with Peritoneal Xenografts. Mol. Ther. Oncolytics *16*, 75–85. https://doi.org/10.1016/j.omto.2019.12.006.

32. Akce, M., Zaidi, M.Y., Waller, E.K., El-Rayes, B.F., and Lesinski, G.B. (2018). The Potential of CAR T Cell Therapy in Pancreatic Cancer. Front. Immunol. *9*, 2166. https://doi.org/10.3389/fimmu.2018.02166.

33. Müller, N., Michen, S., Tietze, S., Töpfer, K., Schulte, A., Lamszus, K., Schmitz, M., Schackert, G., Pastan, I., and Temme, A. (2015). Engineering NK Cells Modified With an EGFRvIII-specific Chimeric Antigen Receptor to Overexpress CXCR4 Improves Immunotherapy of CXCL12/SDF-1alpha-secreting Glioblastoma. J. Immunother. *38*, 197–210. https://doi.org/10.1097/CJI.0000000000000082.

34. Yang, L., Huang, C., Wang, C., Zhang, S., Li, Z., Zhu, Y., Li, D., Gao, L., Ge, Z., Su, M., et al. (2020). Overexpressed CXCR4 and CCR7 on the surface of NK92 cell have improved migration and anti-tumor activity in human colon tumor model. Anti Cancer Drugs *31*, 333–344. https://doi.org/10.1097/CAD.0000000000000868.

35. Raghuwanshi, S.K., Su, Y., Singh, V., Haynes, K., Richmond, A., and Richardson, R.M. (2012). The chemokine receptors CXCR1 and CXCR2 couple to distinct G protein-coupled receptor kinases to mediate and regulate leukocyte functions. J. Immunol. *189*, 2824–2832. https://doi.org/10.4049/jimmunol.1201114.

36. Stadtmann, A., and Zarbock, A. (2012). CXCR2: From Bench to Bedside. Front. Immunol. *3*, 263. https://doi.org/10.3389/fimmu.2012.00263.

37. Shi, X., Wan, Y., Wang, N., Xiang, J., Wang, T., Yang, X., Wang, J., Dong, X., Dong, L., Yan, L., et al. (2021). Selection of a picomolar antibody that targets CXCR2-mediated neutrophil activation and alleviates EAE symptoms. Nat. Commun. *12*, 2547. https://doi.org/10.1038/s41467-021-22810-z.

38. Hassan, R., Thomas, A., Alewine, C., Le, D.T., Jaffee, E.M., and Pastan, I. (2016). Mesothelin Immunotherapy for Cancer: Ready for Prime Time? J. Clin. Oncol. *34*, 4171–4179. https://doi.org/10.1200/JCO.2016.68.3672.

39. Carpenito, C., Milone, M.C., Hassan, R., Simonet, J.C., Lakhal, M., Suhoski, M.M., Varela-Rohena, A., Haines, K.M., Heitjan, D.F., Albelda, S.M., et al. (2009). Control of large, established tumor xenografts with genetically retargeted human T cells containing CD28 and CD137 domains. Proc. Natl. Acad. Sci. USA *106*, 3360–3365. https://doi.org/10.1073/pnas.0813101106.

40. Foeng, J., Comerford, I., and McColl, S.R. (2022). Harnessing the chemokine system to home CAR-T cells into solid tumors. Cell Rep. Med. *3*, 100543. https://doi.org/10.1016/j.xcrm.2022.100543.

41. Rot, A., and von Andrian, U.H. (2004). Chemokines in innate and adaptive host defense: basic chemokinese grammar for immune cells. Annu. Rev. Immunol. *22*, 891–928. https://doi.org/10.1146/annurev.immunol.22.012703.104543.

42. Wennerberg, E., Kremer, V., Childs, R., and Lundqvist, A. (2015). CXCL10-induced migration of adoptively transferred human natural killer cells toward solid tumors causes regression of tumor growth in vivo. Cancer Immunol. Immunother. *64*, 225–235. https://doi.org/10.1007/s00262-014-1629-5.

43. Moustaki, A., Argyropoulos, K.V., Baxevanis, C.N., Papamichail, M., and Perez, S.A. (2011). Effect of the simultaneous administration of glucocorticoids and IL-15 on human NK cell phenotype, proliferation and function. Cancer Immunol. Immunother. *60*, 1683–1695. https://doi.org/10.1007/s00262-011-1067-6.

44. Mailliard, R.B., Alber, S.M., Shen, H., Watkins, S.C., Kirkwood, J.M., Herberman, R.B., and Kalinski, P. (2005). IL-18-induced CD83+CCR7+ NK helper cells. J. Exp. Med. *202*, 941–953. https://doi.org/10.1084/jem.20050128.

45. Lee, Y.E., Go, G.Y., Koh, E.Y., Yoon, H.N., Seo, M., Hong, S.M., Jeong, J.H., Kim, J.C., Cho, D., Kim, T.S., et al. (2023). Synergistic therapeutic combination with a CAF inhibitor enhances CAR-NK-mediated cytotoxicity via reduction of CAF-released IL-6. J. Immunother. Cancer *11*, e006130. https://doi.org/10.1136/jitc-2022-006130.

46. Hassan, R., Bullock, S., Premkumar, A., Kreitman, R.J., Kindler, H., Willingham, M.C., and Pastan, I. (2007). Phase I study of SS1P, a recombinant anti-mesothelin immunotoxin given as a bolus I.V. infusion to patients with mesothelin-expressing mesothelioma, ovarian, and pancreatic cancers. Clin. Cancer Res. *13*, 5144–5149. https://doi.org/10.1158/1078-0432.CCR-07-0869.

47. Gopal, S., Kwon, S.J., Ku, B., Lee, D.W., Kim, J., and Dordick, J.S. (2021). 3D tumor spheroid microarray for high-throughput, high-content natural killer cell-mediated cytotoxicity. Commun. Biol. *4*, 893. https://doi.org/10.1038/s42003-021-02417-2.